

## Facile Assembly of Size- and Shape-Tunable IV–VI Nanocrystals into Superlattices

Yingnan Wang,<sup>†,§</sup> Quanqin Dai,<sup>†,§</sup> Bo Zou,<sup>\*,†</sup> William W. Yu,<sup>\*,‡</sup>  
Bingbing Liu,<sup>†</sup> and Guangtian Zou<sup>†</sup>

<sup>†</sup>State Key Laboratory of Superhard Materials, Jilin University, Changchun 130012, P. R. China, and

<sup>‡</sup>Department of Chemistry and Biochemistry, Worcester Polytechnic Institute, Worcester, Massachusetts 01609, United States. <sup>§</sup>These authors contributed equally to this work.

Received August 30, 2010. Revised Manuscript Received November 3, 2010

In comparison to the previous lengthy approaches, we described a general and simple strategy for engineering the superlattice assembly of IV–VI semiconductor nanocrystals (NCs) with tunable sizes and morphologies. Not only the well-studied spherical NCs but also some special-shaped NCs, such as the quasi-cubic, cubic, truncated octahedral, and octahedral, could self-assemble into well-ordered patterns, as demonstrated in PbS, PbSe, and PbTe. These results extended our proposed model about the configuration of ligand chains in the superlattice assembly. This powerful capability of assembling superlattices was dominated by a heat-treatment process, providing a significant and extensive direction in the engineering of morphology-tunable NC superlattices.

### Introduction

Colloidal nanocrystals (NCs) have been studied extensively for various applications because of their unique size-tunable physical and chemical properties.<sup>1</sup> In practice, to fulfill these extensive applications, much effort tends to utilize NCs as the ideal building block for self-assembling two- and three-dimensional (2D and 3D) superlattice structures. These novel “artificial solids” would provide tunable properties determined by both the properties of individual NC constituents and the collective physical properties of superlattices. Well-defined ordered solids prepared from the tailored nanocrystalline building blocks provide new opportunities to optimize and enhance the nanomaterial properties and performance.<sup>2–5</sup> The achievement of this goal initially requires the building block NCs to be synthesized with quite uniform sizes and shapes. Although great progress on the synthesis of NCs has been made in the past two decades, the design and construction of these NCs superlattices are still a great challenge in material science.

Previous methods for preparing NCs superlattice usually contained lengthy procedures. First, the colloidal NCs were synthesized by the well-developed approaches, e.g., the solution-injected method.<sup>6–8</sup> If the synthesized NCs were of polydispersity, post-synthetic procedures, such as size-selected precipitation<sup>9,10</sup> and

digestive ripening,<sup>11–13</sup> were further used to narrow the size distribution of NCs. That is because the polydispersity in particle sizes was not conducive to the fabrication of well-defined superlattice structures. Subsequently, the monodisperse NCs in a non-polar organic solvent, such as hexane,<sup>14</sup> dodecane,<sup>15</sup> and toluene,<sup>16</sup> were loaded in a glass vial, where a TEM grid was submerged. After several hours/days of solution evaporation, self-assembled NC superlattices would form.<sup>6,17–23</sup> During these formation procedures, other conditions associated with the tilted degree of vials (30°–70°), reduced pressures, and evaporation temperatures (40–100 °C) should be carefully considered.<sup>6,24–26</sup> All of these conditions greatly influenced the final formation of NC superlattices. Obviously, the complicated and time-consuming experimental conditions shown above greatly limit the assembly of NCs into superlattices, triggering the demand for relatively simple approaches to assembling NC superlattices. In our earlier work, we introduced a facile and efficient route to prepare spherical

\*To whom correspondence should be addressed. E-mail: zoub@jlu.edu.cn (B.Z.); wyu@wpi.edu (W.W.Y.).

- (1) Peng, X. G.; Manna, L.; Yang, W. D.; Wickham, J.; Scher, E.; Kadavanich, A.; Alivisatos, A. P. *Nature* **2000**, *404*, 59–61.  
(2) Urban, J. J.; Talapin, D. V.; Shevchenko, E. V.; Murray, C. B. *J. Am. Chem. Soc.* **2006**, *128*, 3248–3255.  
(3) Zaitseva, N.; Dai, Z. R.; Leon, F. R.; Krol, D. *J. Am. Chem. Soc.* **2005**, *127*, 10221–10226.  
(4) Kalsin, A. M.; Fialkowski, M.; Paszewski, M.; Smoukov, S. K.; Bishop, K. J. M.; Grzybowski, B. A. *Science* **2006**, *312*, 420–424.  
(5) Wang, Z. L. *Adv. Mater.* **1998**, *10*, 13–30.  
(6) Shevchenko, E. V.; Talapin, D. V.; Murray, C. B.; O'Brien, S. *J. Am. Chem. Soc.* **2006**, *128*, 3620–3637.  
(7) Yu, W. W.; Peng, X. G. *Angew. Chem., Int. Ed.* **2002**, *41*, 2368–2371.  
(8) Dai, Q. Q.; Wang, Y. N.; Zhang, Y.; Li, X. B.; Li, R. W.; Zou, B.; Seo, J. T.; Wang, Y. D.; Liu, M. H.; Yu, W. W. *Langmuir* **2009**, *25*, 12320–12324.  
(9) Korgel, B. A.; Fitzmaurice, D. *Adv. Mater.* **1998**, *10*, 661–665.  
(10) Shevchenko, E. V.; Talapin, D. V.; Rogach, A. L.; Kornowski, A.; Haase, M.; Weller, H. *J. Am. Chem. Soc.* **2002**, *124*, 11480–11485.

- (11) Yang, Y.; Liu, S.; Kimura, K. *Angew. Chem., Int. Ed.* **2006**, *45*, 5662–5665.  
(12) Stoeva, S. I.; Klabunde, K. J.; Sorensen, C. M.; Dragieva, I. *J. Am. Chem. Soc.* **2002**, *124*, 2305–2311.  
(13) Stoeva, S. I.; Prasad, B. L. V.; Uma, S.; Stoimenov, P. K.; Zaikovski, V.; Sorensen, C. M.; Klabunde, K. J. *J. Phys. Chem. B* **2003**, *107*, 7441–7448.  
(14) Sun, S. *Adv. Mater.* **2006**, *18*, 393–403.  
(15) Martin, J. E.; Wilcoxon, J. P.; Odinek, J.; Provencio, P. *J. Phys. Chem. B* **2002**, *106*, 971–978.  
(16) Shevchenko, E. V.; Talapin, D. V.; Kornowski, A.; Wieshorst, F.; Kotzler, J.; Haase, M.; Rogach, A. L.; Weller, H. *Adv. Mater.* **2002**, *14*, 287–290.  
(17) Sun, S. H.; Murray, C. B. *J. Appl. Phys.* **1999**, *85*, 4325–4330.  
(18) Wang, D. S.; Xie, T.; Peng, Q.; Li, Y. D. *J. Am. Chem. Soc.* **2008**, *130*, 4016–4022.  
(19) Song, Q.; Ding, Y.; Wang, Z. L.; Zhang, Z. *J. Phys. Chem. B* **2006**, *110*, 25547–25550.  
(20) Lu, W. G.; Liu, Q. S.; Sun, Z. Y.; He, J. B.; Ezeolu, C.; Fang, J. Y. *J. Am. Chem. Soc.* **2008**, *130*, 6983–6991.  
(21) Yin, M.; O'Brien, S. *J. Am. Chem. Soc.* **2003**, *125*, 10180–10181.  
(22) Kang, C. C.; Lai, C. W.; Peng, H. C.; Shyue, J. J.; Chou, P. T. *ACS Nano* **2008**, *2*, 750–756.  
(23) Kovalenko, M. V.; Heiss, W.; Shevchenko, E. V.; S. Lee, J.; Schwinghammer, H.; Alivisatos, A. P.; Talapin, D. V. *J. Am. Chem. Soc.* **2007**, *129*, 11354–11355.  
(24) Talapin, D. V.; Shevchenko, E. V.; Murray, C. B.; Titov, A. V.; Kral, P. *Nano Lett.* **2007**, *7*, 1213–1219.  
(25) Chen, Z. Y.; Moore, J.; Radtke, G.; Sirringhaus, H.; O'Brien, S. *J. Am. Chem. Soc.* **2007**, *129*, 15702–15709.  
(26) Lu, C. G.; Chen, Z. Y.; O'Brien, S. *Chem. Mater.* **2008**, *20*, 3594–3600.

PbSe NC superlattices and demonstrated that the configuration of capping ligand chains strongly related to the natural cooling of reactions played the dominant role in assembling spherical PbSe NCs into periodic superlattice structures.<sup>27</sup> Additionally, it should be emphasized that most 2D and 3D superlattices achieved so far were composed of spherical NCs. It has been rarely reported that NCs, especially IV–VI NCs, with other shapes, such as octahedron,<sup>20,21</sup> cube,<sup>28</sup> and truncated octahedron,<sup>29,30</sup> have the ability to construct 2D and 3D superlattices.

In this paper, we extend our simple and reproducible method established on the basis of spherical PbSe NC superlattices<sup>27</sup> to prepare superlattices of size and shape-tunable IV–VI (PbS, PbSe, and PbTe) NCs. These near- to mid-infrared-emitting nanomaterials have been widely studied for solar-cell,<sup>31–33</sup> telecommunication,<sup>34</sup> optical switches,<sup>35</sup> field effect transistors (FET),<sup>36</sup> and biological applications<sup>37,38</sup> because of their narrow direct band gaps (0.28–0.41 eV) and large exciton Bohr radii (18–46 nm). Although there are many reports on the synthesis of colloidal PbS, PbSe, and PbTe NCs,<sup>39–45</sup> there lack efficient methods to assemble them into periodic superlattices, especially the superlattices composed of morphology-tunable NCs. A facile method is presented here to prepare the superlattices of size- and shape-tunable IV–VI NCs, including the well-developed spherical morphology and the less-known quasi-cubic, cubic, truncated octahedral, and octahedral shapes. This size and shape-tunable ability was achieved by simply varying the reaction temperature, reaction time, and surfactants. In our experiments, the hot colloidal solution was cooled naturally in the three-necked flask or Teflon-lined autoclaves, and such naturally cooled NCs could spontaneously assemble into highly ordered superlattices on the TEM grids. Moreover, compared with previous methods, our approach for preparing NC superlattices did not need many experimental conditions, such as tilted degree of vials, reduced pressures, and evaporation temperatures. Instead, all the obtained NC colloidal solutions were directly dropped on TEM grids in the air. Meanwhile, the NC superlattice structures were formed quickly.

## Experiment

**Materials.** Trioctylphosphine (TOP, technical grade 90%), 1-octadecene (ODE, technical grade 90%), selenium powder

- (27) Wang, Y. N.; Dai, Q. Q.; Wang, L. C.; Zou, B.; Cui, T.; Liu, B. B.; Yu, W. W.; Hu, M. Z.; Zou, G. T. *J. Phys. Chem. C* **2010**, *114*, 11425–11429.
- (28) Li, F.; Delo, S. A.; Stein, A. *Angew. Chem., Int. Ed.* **2007**, *46*, 6666–6669.
- (29) Wang, Z. L. *J. Phys. Chem. B* **2000**, *104*, 1153–1175.
- (30) Zheng, R.; Gu, H.; Xu, B.; Fung, K. K.; Zhang, X.; Ringer, S. P. *Adv. Mater.* **2006**, *18*, 2418–2421.
- (31) McDonald, S. A.; Konstantatos, G.; Zhang, S.; Cyr, P. W.; Klem, E. J. D.; Levina, L.; Sargent, E. H. *Nature Mater.* **2005**, *4*, 138–142.
- (32) Koleilat, G. I.; Levina, L.; Shukla, H.; Myrskog, S. H.; Hinds, S.; Pattantyus-Abraham, A. G.; Sargent, E. H. *ACS Nano* **2008**, *2*, 833–840.
- (33) Law, M.; Beard, M. C.; Choi, S.; Luther, J. M.; Hanna, M. C.; Nozik, A. J. *Nano Lett.* **2008**, *8*, 3904–3910.
- (34) Harrison, M. T.; Kershaw, S. V.; Burt, M. G.; Rogach, A. L.; Kornowski, A.; Eychmuller, A.; Weller, H. *Pure Appl. Chem.* **2000**, *72*, 295–307.
- (35) Wise, F. W. *Acc. Chem. Res.* **2000**, *33*, 773–780.
- (36) Talapin, D. V.; Murray, C. B. *Science* **2005**, *310*, 86–89.
- (37) Weissleder, R. *Nature Biotechnol.* **2001**, *19*, 316–317.
- (38) Medintz, I. L.; Goldman, E. R.; Uyeda, H. T.; Mattoussi, H. *Nature Mater.* **2005**, *4*, 435–446.
- (39) Murphy, J. E.; Beard, M. C.; Norman, A. G.; Ahrenkiel, S. P.; Johnson, J. C.; Yu, P. R.; Mićić, O. I.; Ellingson, R. J.; Nozik, A. J. *J. Am. Chem. Soc.* **2006**, *128*, 3241–3247.
- (40) Mokari, T.; Zhang, M.; Yang, P. D. *J. Am. Chem. Soc.* **2007**, *129*, 9864–9865.
- (41) Lu, W. G.; Fang, J. Y.; Ding, Y.; Wang, Z. L. *J. Phys. Chem. B* **2005**, *109*, 19219–19222.
- (42) Lu, W. G.; Fang, J. Y.; Stokes, K. L.; Lin, J. J. *Am. Chem. Soc.* **2004**, *126*, 11798–11799.
- (43) Abel, K. A.; Shan, J. N.; Boyer, J. C.; Harris, F.; van Veggel, F. J. M. *Chem. Mater.* **2008**, *20*, 3794–3796.

(100 mesh, 99.5%), lead oxide (99.999%), PbCl<sub>2</sub> (99.999%), sulfur powder (99.98%), tellurium powder (99.99%), oleic acid (OA, technical grade 90%), trioctylamine (98%), oleylamine (OLA, 70%), and octylamine (99%) were purchased from Aldrich. Methanol, toluene, ethanol, tetrachloroethylene (TCE), and acetone were obtained from commercial sources. All chemicals were used as received without further purification.

**Synthesis of PbSe NCs and Their Superlattices.** Typically, a mixture of PbO powder (0.0558 g, 0.25 mmol), oleic acid (0.5 mL), and ODE (5.0 mL) was added to a 50 mL three-neck flask. This mixture was heated to 120 °C under a nitrogen flow, where yellow PbO powder was completely dissolved under stirring. After the mixture was naturally cooled to room temperature, 1.5 mL of 1.67 M TOP-Se solution prepared in a glovebox was added into the flask, and then the temperature was reheated up to 150 °C and maintained for 1 h. After that, the heating mantle was turned off, so that the colloidal NC solution could be naturally cooled down to room temperature (about 1–2 h). Transmission electron microscopy (TEM) was employed to determine whether the as-synthesized samples above could finally self-assemble into periodically arranged superlattices or still appeared random on the TEM grid. Prior to TEM measurements, the obtained crude room-temperature PbSe solutions needed to be purified as follows. An equal volume of methanol to the crude sample solution was added to extract the sample; then the extracted PbSe sample was precipitated with excess acetone; and finally this residual sample was redispersed in TCE and dropped on copper grids for the TEM characterization. Such purification procedures and TEM characterizations were also used in all the cases shown below.

**Synthesis of PbTe NCs and Their Superlattices.** Typically, PbO (0.223 g, 1.0 mmol), oleic acid (2.0 mL), and ODE (5.0 mL) were loaded into a three-neck flask and heated to 120 °C to dissolve PbO powder under a N<sub>2</sub> flow. After the mixture was naturally cooled to room temperature, 1.0 mL of 0.5 M TOP-Te solution was added into the flask, and then the temperature was brought up to 180 °C and maintained for 10 min. After that, the heating mantle was turned off, and the colloidal NC solution was naturally cooled down to room temperature (about 1–2 h).

**Synthesis of PbS NCs and Their Superlattices.** Typically, PbO (0.223 g, 1.0 mmol), oleic acid (2.0 mL), and trioctylamine (5 mL) were loaded into a 50 mL three-necked flask. The mixture was heated to 120 °C until the Pb–oleate complex formed. After the mixture was naturally cooled to room temperature, 3.4 mL of 0.1 M sulfur solution (including sulfur and a mixture of oleylamine and phenyl ether with a 1:4 volume ratio of oleylamine to phenyl ether) was added. After being stirred for a few minutes, the above homogeneous solution was heated to 150 °C and kept for 0.5 h. Afterward, the heating mantle was turned off, where the colloidal NC solution could naturally cool down to room temperature (about 1–2 h).

**Characterization.** All measurements were performed at room temperature. A Hitachi H-8100IV transmission electron microscope operating at 200 kV was used to take TEM images. Near-infrared absorption spectra were monitored by a Shimadzu UV-3150 spectrometer. X-ray diffraction (XRD) patterns were recorded via a Bruker D8 diffractometer working with a Cu K $\alpha$  target.

## Results and Discussion

**Synthesis of IV–VI NCs.** As the building block for assembling superlattice structures, the monodisperse NCs should be prepared first. In our experiments, the standard deviations ( $\delta$ ) of these NC sizes were calculated to be 5–8% (Figure S1). TEM images shown in Figure 1 revealed that all the prepared IV–VI NCs (PbS, PbSe, and PbTe) with different shapes were highly

- (44) Wang, X.; Zhuang, J.; Peng, Q.; Li, Y. D. *Langmuir* **2006**, *22*, 7364–7368.
- (45) Xu, J.; Ge, J. P.; Li, Y. D. *J. Phys. Chem. B* **2006**, *110*, 2497–2501.

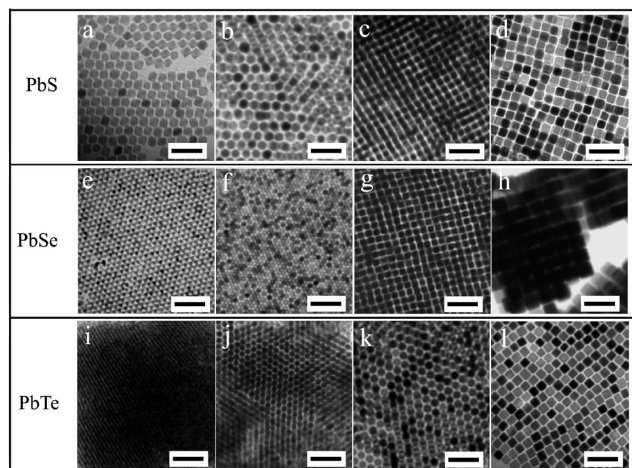


**Figure 1.** TEM images of IV–VI NC superlattices. All scale bars represent 50 nm.

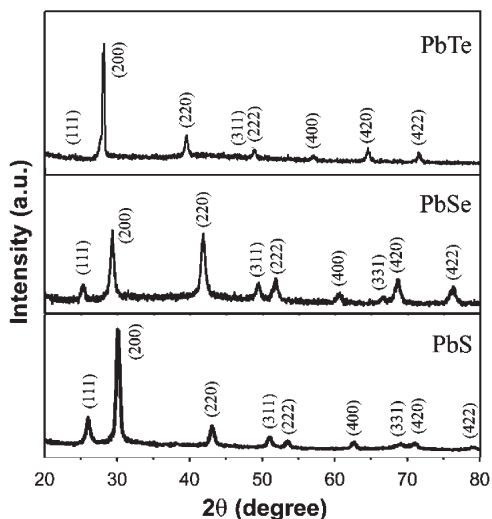


**Figure 2.** X-ray diffraction patterns of the as-prepared cubic PbS, PbSe, and PbTe NC samples.

uniform in both sizes and shapes. For the preparation of NC superlattices, the building block of NCs should be quite uniform in sizes and shapes, which is one of the most important prerequisites. The X-ray diffraction (XRD) analysis of the whole sample indicated that all diffraction peaks could be easily indexed to the cubic rock salt PbS (JCPDS 05-0592), PbSe (JCPDS 78-1903), and PbTe (JCPDS 38-1435), as shown in Figure 2. By applying the Debye–Scherrer equation to the line broadening of the (200) peak, the particle sizes were estimated to be 14.0 nm (PbS), 21.0 nm (PbSe), and 15.0 nm (PbTe), which was consistent with the TEM measurements in Figure 1d,h,l.

It was previously reported that lead chalcogenide NCs could evolved from nanosphere/polyhedron to nanocube, undergoing a shape evolution with the alteration of reaction parameters, such as growth temperature and reaction time.<sup>39–42,46</sup> That is because, for the rock salt structure of IV–VI nanocrystals, the growth of the higher surface energy (111) face in the ⟨111⟩ direction was faster than that of the lower surface energy (100) face in the ⟨100⟩ direction. This would favor the growth of the (111) facets, resulting in the formation of cubic-like nanostructures with the

lowest total surface energy.<sup>39,42</sup> Among the reaction parameters, we found that mixing precursors (e.g., TOP-Se and Pb-oleate) at different temperatures could be used to control the size and even shape of IV–VI NCs (Table S1). We used two ways in our experiments to mix the precursors: the precursors were mixed at room temperature and then directly heated up to a specific reaction temperature, namely heating up (HU); comparatively, injecting the chalcogenide precursor into the Pb-oleate precursor at high temperatures was named hot injection (HI). The main difference between these two ways is the different injection temperature of precursors. From our experimental results, we noted that the higher the injection temperature of precursors, the easier the large size of IV–VI NCs could be obtained. This phenomenon was monitored by absorption spectra. Taking the case of PbSe NCs as a sample, if the TOP-Se solution was injected into the 150 °C Pb-oleate precursor, ~6.0 nm PbSe NCs could be obtained when the reaction was lasted for 9 min (Figure 3). Comparatively, it took 60 min to produce the same-size PbSe NCs if the TOP-Se was added into the room-temperature Pb-oleate precursor and then reheated to 150 °C. Therefore, it was easy to use the HI route to produce large-size cubic-like IV–VI NCs with narrow size distribution (Figures 1h,l and 3b), while the HU method was suitable for synthesis of small-size NCs.

In addition, changing the lead source, capped ligand, and reaction solvent could also be used to synthesize size and shape-tunable IV–VI NCs. Typically, capped ligands with a large hydrocarbon chain generated smaller particles due to the slower nucleation and growth rate.<sup>47</sup> For example, in the case of PbS NCs, when octylamine was used as the capped ligand instead of trioctylamine, ~16 nm cubic PbS NCs were obtained at 100 °C (Figure 1d). When PbCl<sub>2</sub> was used as the lead source instead of PbO, ~10 nm quasi-cubic PbS NCs could be obtained at 240 °C for 60 min (Figure 1c).

**Self-Assembly of IV–VI NCs and Their Assembly Mechanism.** Previously, the synthesis of IV–VI NCs by the HI method was generally accompanied by a quick quenching process, resulting in monodisperse and random NCs.<sup>39–43,48</sup> However, in our synthesis, all the crude NCs in reaction vessels (three-neck flask or Teflon-lined autoclave) were naturally cooled to room temperature, instead of the traditional quick quenching process. Surprisingly, our naturally cooled NCs without any lengthy treatment could assemble into well-ordered superlattices when they were dropped on the TEM grids. In contrast, if IV–VI NCs synthesized in the reaction vessel was quickly quenched to room temperature, these NCs appeared monodisperse without any ordered arrangement (Figure S2). Our experimental results above revealed that our simple self-assembly of NC superlattices was closely associated with the natural cooling process. Other factors, including the role of solvents, different carrier solutions, NC concentrations, solvent evaporation rate, and different capped ligands were taken into account in our recent work, indicating that these factors had almost no effect on the assembling process of superlattices.<sup>27</sup> In short, after these size- and shape-uniform NCs were synthesized at high temperatures, these NCs could spontaneously assemble on TEM grids if they were naturally cooled to room temperature. Moreover, with the increase of NCs concentration, the large NCs assembling area could be obtained, and this large area NCs superlattice further indicated that the obtained NCs were highly uniform in both sizes and shapes (Figure 4). The corresponding formation mechanism of IV–VI NC superlattices is discussed below.

(46) Wang, Y. N.; Dai, Q. Q.; Yang, X. Y.; Zou, B.; Li, D. M.; Liu, B. B.; Hu, M. Z.; Zou, G. T. *CrystEngComm* **2010**, DOI: 10.1039/C004459H.

(47) Peng, Z. A.; Peng, X. G. *J. Am. Chem. Soc.* **2001**, *123*, 1389–1395.

(48) Yu, W. W.; Falkner, J. C.; Shih, B. S.; Colvin, V. L. *Chem. Mater.* **2004**, *16*, 3318–3322.

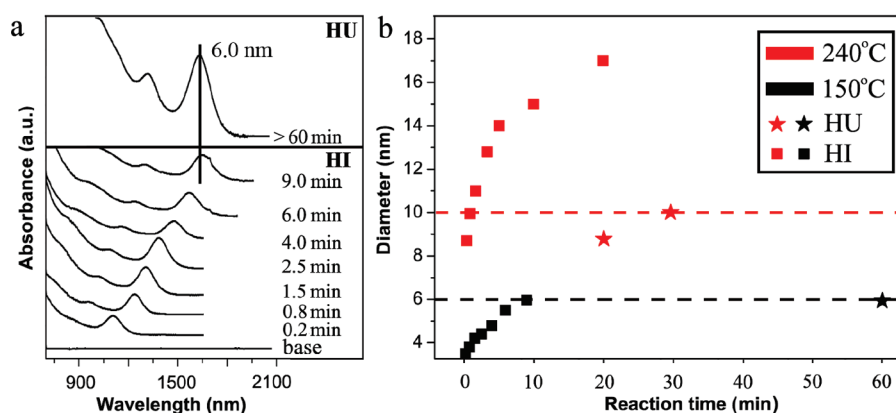


**Figure 3.** Comparison between the heating-up (HU) method and hot-injection (HI) method, taking the case of synthesizing PbSe NCs as an example. (a) Near-infrared absorption spectra of the PbSe NCs synthesized at 150 °C. (b) The size of PbSe NCs versus reaction time and temperature.

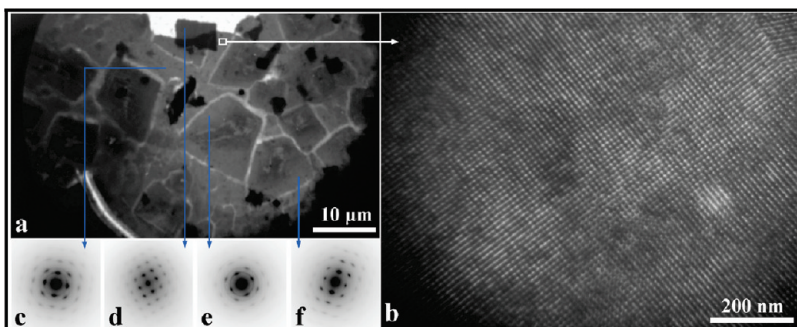


**Figure 4.** (a, b) Low- and high-magnification TEM images of ~10 nm PbSe NCs superlattices, respectively. (c–f) Select region wide-angle electron diffraction (WED) patterns.

The fabrication of NC superlattices was previously attributed to many driving forces, especially entropy and ligand–ligand interactions as the dominant roles.<sup>25</sup> In the hard-sphere model, the entropy-driven process can be rationalized into two types: the configurational entropy and free volume entropy. In this case, the system favors to adopt the NCs superlattice structure with the most efficient space-filling, i.e., face-centered cube (fcc, ABCABC-type stacking) and hexagonal (hcp, ABAB-type stacking) close packing. With regard to ligand–ligand interactions, Wang et al. observed the bundling and interdigititation of thiolate molecules in the self-assembly of Ag NC superlattices.<sup>49</sup> Schliehe and co-workers showed that the formation of ordered and densely packed ligand surface layers of oleic acid on {100} PbS surfaces could drive the normally isotropic crystal growths into a 2D oriented attachment of NCs. Moreover, this highly ordered monolayer oleic acid molecules monolayer further make these 2D PbS sheets assemble into stacking.<sup>50</sup> Iwahashi et al. indicated that the short alkyl chains could become ordered with the gradual decrease of temperature and clusters of quasi-smectic liquid crystal could readily form below 30 °C.<sup>51</sup> In addition to these experimental results, molecular dynamics simulation in previous other works not only indicated that the orientationally ordered structure of chain molecules would form with the gradual decrease of temperature<sup>52,53</sup>

but also demonstrated that the capping ligand of NCs played the dominant role during their self-assembling processes.<sup>54</sup> Via introducing a model of the configuration of capping ligand chains, we earlier explained the formation process of assembling spheric PbSe NCs into their superlattices on the basis of a series of experiments and molecular dynamics simulations.<sup>27</sup> After the monodisperse PbSe NCs capped with appropriate ligand chains were synthesized at high temperatures, these crude PbSe NCs were cooled naturally in the reaction vessel instead of the quick quenching process. Accordingly, the orientational configuration of capped ligand chains would form with the gradual decrease of temperature, resulting in an order state of ligand chains at room temperature. At such a state, NCs were interacting and thus showed orderly arranged superlattice structures, which was attributed to solvent evaporation-induced ligand–ligand van der Waals (VDW) interaction and entropy driving process (Figure 5). Comparatively, when the crude PbSe NCs were quickly quenched to room temperature, their ligand chains were captured in a disordered state. According to the Salem expression,<sup>55</sup> when the ligand chains were in a random and disordered configuration, the interactions of ligand–ligand VDW interaction were so weak that the corresponding NCs were noninteracting and randomly arranged. In fact, the elevated temperature and reduced pressure evaporation process in the traditional fabrication of NC superlattices were used to make the capping ligand chains become ordered. This complicated manipulation was simplified and achieved by the natural cooling process shown in our experiments. Therefore, no

(49) Wang, Z. L.; Harfenist, S. A.; Whetten, R. L.; Bentley, J.; Evans, N. D. *J. Phys. Chem. B* **1998**, *102*, 3068–3072.

(50) Schliehe, C.; Juarez, B. H.; Pelletier, M.; Jander, S.; Greshnykh, D.; Nagel, M.; Meyer, A.; Foerster, S.; Kornowski, A.; Klinke, C.; Weller, H. *Science* **2010**, *329*, 550–553.

(51) Iwahashi, M.; Yamaguchi, Y.; Kato, T.; Horiuchi, T.; Sakurai, I.; Suzuki, M. *J. Phys. Chem.* **1991**, *95*, 445–451.

(52) Fujiwara, S.; Sato, T. *Phys. Rev. Lett.* **1998**, *80*, 991–994.

(53) Fujiwara, S.; Sato, T. *J. Chem. Phys.* **1999**, *110*, 9757–9764.

(54) Schapotschnikow, P.; van Huis, M. A.; Zandbergen, H. W.; Vanmaekelbergh, D.; Vlugt, T. H. *Nano Lett.* **2010**, *10*, 3966–3971.

(55) Salem, L. *J. Chem. Phys.* **1962**, *37*, 2100–211.

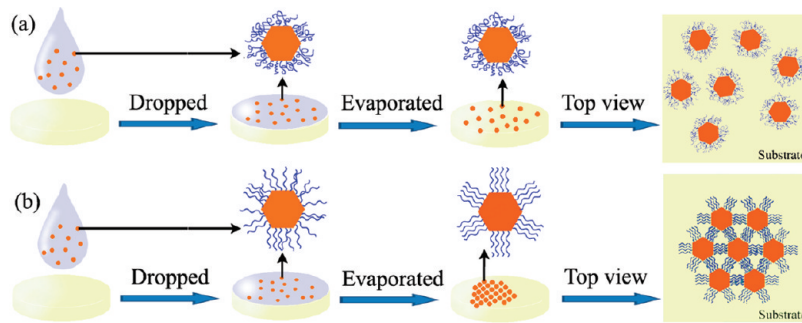


**Figure 5.** Schematic illustration of prepare random monodisperse NCs and NCs superlattices: (a) NCs which were quenched by toluene and redispersed in TCE; (b) NCs which were naturally cooled to RT and redispersed in TCE.

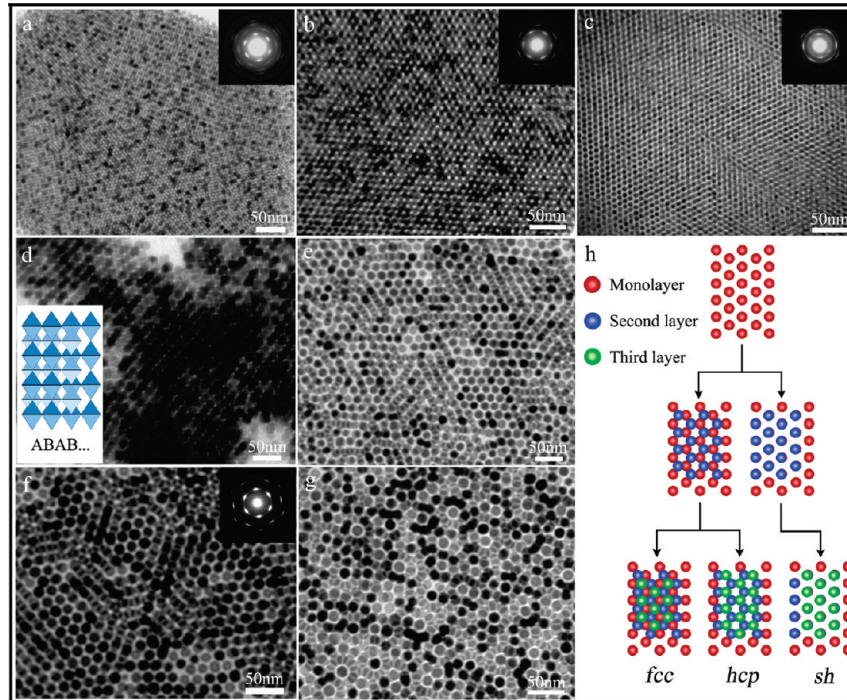


**Figure 6.** TEM images of spherical and faceted IV–VI NCs superlattices. (a) fcc lattice and (b) hcp lattice of 8.5 nm PbSe NCs and (c) sh lattice of 6.0 nm PbSe NCs, respectively. (d, e) TEM images of multilayer self-assembly patterns which were prepared with  $\sim$ 14.0 nm octahedral and  $\sim$ 14.5 nm truncated octahedral PbS NCs. (f, g) Different patterns of  $\sim$ 12.5 nm PbTe NCs. (h) Schematic depiction of spherical or faceted NC packing in different periodic structures. The insets in panels a, b, c, and f show wide-angle electron diffraction patterns of the corresponding superlattices. The inset schematics in panel d indicate hcp stacking of octahedral PbS NCs.

matter what shapes of the IV–VI NCs, they could readily self-assemble into well-ordered patterns via the natural cooling process.

**Spherical and Faceted IV–VI NCs Superlattices.** Generally, the configurational entropy and free volume entropy favor the assembly of spherical NCs into their superlattice structures with the highest packing density via the fcc and hcp packing. Moreover, NCs of diluent concentrations easily arranged into ordered monolayers; such arrangements typically show hexagonal packing, corresponding to a maximal packing density of spherical or faceted NCs (Figure S3). The difference between fcc and hcp structures was determined by the location of NCs in the third layer, where spherical and faceted IV–VI NCs could grow layer-by-layer and show the fcc and hcp packing (Figure 6 and Figure S4). In addition to the fcc and hcp packing structures, spherical and faceted IV–VI NCs often self-assembled into the sh packing, which could be explained by considering the interactions between nonlocal dipoles of individual NCs.<sup>24</sup> Figure 6c showed the TEM image of PbSe NC superlattices, self-assembling along the [001] projection of sh packing lattices. The layers were composed of

NCs with the hexagonal ordering, and assembled (at least a three-layer thickness) in the vertical direction. The  $60^\circ$  angle between the lattice planes (Figure S5a) indicated the PbSe NC superlattice exhibited a typical hexagonal arrangement of NCs. Further investigation of this PbSe NC superlattice showed that there existed other different projections of fcc lattices (such as [011], [100], [010]), which are displayed in Figure S5b–d. The  $70.5^\circ$  angle between the planes of the fcc lattice marked in Figure S5b is consistent with the [011] projection. The corresponding wide-angle electron diffraction (WED) also indicated that the NCs were organized regularly. Similarly, spherical or faceted PbS and PbTe NCs could also arranged into these typical periodic patterns (Figure 6d–h). In addition, when octahedral PbS NCs self-assembled into the monolayer arrangement, the pattern was stabilized by both placing the NC [110] facets on the substrate and supporting each other through the maximum contact on the [111] facets of adjacent NCs (Figure 1a). However, when the superlattices of octahedral PbS NCs were extended to multilayer patterns (Figure 6d), the octahedral NCs would sit on a [110] facet and were supported by

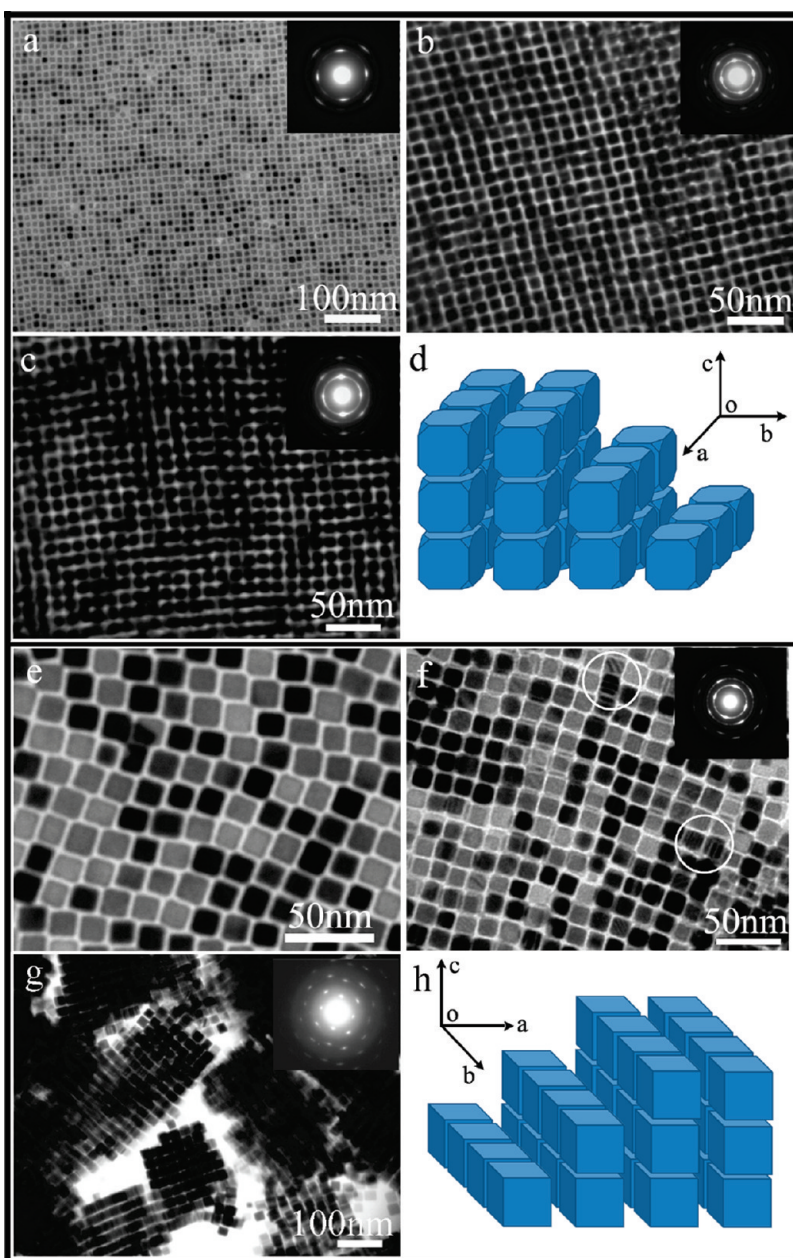


**Figure 7.** TEM images of quasi-cubic and cubic IV–VI NCs superlattices. (a, b) Monolayer and multilayer well-ordered  $\sim 10.0$  nm quasi-cubic PbSe NCs. (c) Multilayer superlattice arranged by  $\sim 10.0$  nm quasi-cubic PbS NCs. (d) Structure model showing simple-cubic (sc) stacking by quasi-cubic NCs. (e) TEM image of monolayer patterns assembled with  $\sim 16.0$  nm cubic PbTe NCs. (f) Multilayer superlattice of  $\sim 16.0$  nm cubic PbS NCs. The marked regions show moiré fringes. (g) Multilayer superlattice of  $\sim 21.0$  nm cubic PbSe NCs. (h) Structure model showing simple-cubic (sc) stacking by cubic NCs. The insets in panels a, b, c, f, and g show wide-angle electron diffraction patterns of the corresponding superlattices.

contacting two vertices of two adjacent NCs in the first row. To further stabilize this pattern, NCs built in the next row had to contact their vertical [110] edges with those of their nearest-neighbor NCs.<sup>20</sup> Therefore, these layers exhibit ABAB..., typical hcp-type stacking (see the inserted structure model in Figure 6d).

**Quasi-Cubic and Cubic IV–VI NC Superlattices.** Although the monodisperse quasi-cubic or cubic IV–VI NCs were successfully synthesized in previous approaches,<sup>39–42,46</sup> these advanced morphologies have been rarely reported in the assembly of the superlattice structures. Similar to the spherical and faceted IV–VI NCs shown above, different concentrations of the quasi-cubic and cubic NCs could also arrange into different periodic patterns, including monolayer well-ordered structures (Figure 7a,e) and multilayer structures with the simple-cubic (sc) packing lattice

(Figure 7b,c), fcc lattice, and distorted hcp lattice (Figure S6). These quasi-cubic NCs that formed layers could be indexed as a primitive cube (Figure 7d), where the layers assembled one-by-one in the vertical direction (i.e., AAA-type layer stacking). In addition, the quasi-cubic NCs arranged into square superlattice islands, compared to the round islands of spherical NCs (Figure S7). With regard to the cubic NCs, their self-assembled patterns tended to exhibit exclusive sc-type stacking. Figure 7f shows that cubic PbS NCs were well-ordered with the sc-type stacking, as confirmed by WED patterns. Because of electron diffractions in the double-layer NCs with mutually rotated atoms, lattice planes gave rise to rotational moiré fringes which could be clearly observed (marked in Figure 7f). Similarly, the same sc-type stacking could be also observed in the cubic PbSe NCs (Figure 7g). The

WED pattern indicated these cubic PbSe NCs arranged well and exhibited a 4-fold symmetry. From the patterns of IV–VI NC superlattices, we noted that quasi-cubic and cubic IV–VI NCs tended to self-assemble into the sc packing structures, while spherical and faceted IV–VI NCs favorably self-assembled into fcc and hcp packing structures.

### Conclusion

In conclusion, size- and shape-tunable IV–VI (PbS, PbSe, and PbTe) NCs were synthesized and subsequently naturally cooled down to room temperature. This natural cooling process made the synthesized NCs capped with ordered ligand chains, thereby showing spontaneously assembled superlattice patterns on the TEM grid without any other postsynthetic procedures. This spontaneous assembly was attributed to solvent evaporation-induced ligand–ligand VDW interaction and entropy-driven

force, further proving our configuration model of ligand chains. It is not unreasonable to further believe that this model and approach can significantly be extended to prepare superlattices of other NCs (Figure S8).

**Acknowledgment.** This work was supported by NSFC (Nos. 21073071, 51025206, and 10979001) and the National Basic Research Program of China (Nos. 2011CB808200 and 2007CB808000).

**Supporting Information Available:** Additional TEM images of IV–VI NC superlattices and a table regarding precursors, capping ligands, reaction temperature, and time used in the synthesis of IV–VI semiconductor NCs. This material is available free of charge via the Internet at <http://pubs.acs.org>.